Heat Transfer Research 45(1), 75–95 (2014)

MIXED CONVECTION HEAT TRANSFER IN A DOUBLE LID-DRIVEN INCLINED SQUARE ENCLOSURE SUBJECTED TO Cu–WATER NANOFLUID WITH PARTICLE DIAMETER OF 90 nm

Mohammad Reza Heydari,[1] Mohammad Hemmat Esfe,[2,] Mohammad Hadi Hajmohammad,[2] Mohammad Akbari,[2] & Seyed Sadegh Mirtalebi Esforjani[2]*

[1]*Parand Branch, Islamic Azad University, Tehran, Iran*

[2]*Department of Mechanical Engineering, Najafabad Branch, Islamic Azad University, Isfahan, Iran*

[*]Address all correspondence to Mohammad Hemmat Esfe
E-mail: M.hemmatesfe@gmail.com

In this article, mixed convection flow in a two-sided lid-driven cavity at different inclination angles filled with Cu–water nanofluid (with diameter of 90 nm) is studied numerically using the finite volume method. For different values of solid volume fraction of nanoparticles, flow is induced by the top and right-hand sidewalls sliding at constant speed. The left-hand sidewall is kept constant at higher temperature (T_h), while the right moving wall is maintained at a lower temperature (T_c), thereby introducing natural convection. In this study, bottom and top walls were assumed isolated; Richardson number ranged from 0.001 to 10, nanoparticles solid volume fraction (φ) up to 0.06 were investigated, and cavity inclination angle from 0° to 90° was considered and the Grashof number was set to 10^4. The influence of inclination angle and φ of the nanofluids on hydrodynamic and thermal characteristics is discussed. The results indicated that increase in φ for a constant Ri enhances heat transfer. Also, heat transfer was increased as Ri was decreased for a particular φ. Moreover, where natural convection is dominant (i.e., higher Ri), the flow form seems to be influenced more by φ.

KEY WORDS: *nanofluid, heat transfer, mixed convection, double lid-driven cavity, numerical analysis*

1. INTRODUCTION

Many fluids traditionally used for heat transfer (e.g., water and mineral oils) have rather low thermal conductivities. Considering the ever-increasing demand for fluids

1064-2285/14/$35.00

with superior heat transfer performance, fluids with nano-scale conductive particles have become the subject of intense research among academics within the last two decades. Choi (1995), who suggested such fluids for the first time in the mid-1990s, referred to them as nanofluids, and a large number of studies involving analytical, numerical, and experimental evidence have been published ever since. Masuda et al. (1993) reported a 20% increase in the effective thermal conductivity of ethylene glycol as a result of adding just 0.3% volume fraction suspended nanoparticles. Nanofluids containing ceramic oxides in water have also been shown to enhance thermal conductivity (Lee et al., 1999) where Al_2O_3 nanoparticles with a mean diameter of 13 nm at 4.3% volume fraction increased thermal conductivity by 30% compared to water.

Other researchers have studied shape, size, and thermal properties of the solid particles in nanofluids and investigated their influence on thermal conductivity (Xuan and Li, 2000). As regards the size, small particles have been shown to enhance heat transfer capability and stability (Hwang et al., 2007) as compared with larger particles. A cavity filled with nanofluid has also been studied by several researchers due to their applications. Hwang et al. (2007) developed a numerical model to evaluate natural convection heat transfer in a rectangular cavity heated from below using Al_2O_3 nanofluid. They utilized various models to obtain the effective thermal conductivity and viscosity. Their results indicated that base fluid is more unstable than Al_2O_3 nanofluids in a rectangular cavity. Also, stability increases when the volume fraction (φ) of nanofluid increases, or nanoparticle size decreases, or the average temperature of nanofluids increases. Using water–TiO_2 nanofluid, Wen and Ding (2006) in another study showed that for Rayleigh numbers (Ra) less than 10^6, increasing nanoparticle concentration reduced the natural convection heat transfer rate at a particular Ra. Numerical simulation of natural convection in a cavity filled with nanofluid has also been examined by Khanafer et al. (2003), where nanofluid in the cavity was considered to be in single phase. The impact of nanoparticle concentration on the buoyancy-driven heat transfer process was discussed. Consequently, at any given Grashof number (Gr), the heat transfer rate increases as φ is increased.

Mixed convection flows (i.e., combination of both natural and forced convection) is a complex phenomenon because of the interaction of buoyancy and shear forces and occurs in industrial applications such as cooling of electronic devices, food processing, crystal growth, lubrication technologies, drying technologies, and chemical processing equipment (Basak et al., 2009; Guo and Sharif, 2004; Quertatani et al., 2009). Mixed convection in a square ventilation cavity subjected to a nanofluid at different values of Ri was studied numerically by Shahie et al. (2010), who reported the impact of the presence of nanoparticles on the hydrodynamic and thermal characteristics of flow. Recently, lid-driven cavity has attracted a great deal of attention owing to their extensive industrial applications. Mohammad and Viskanta (1992) studied the impact of a sliding wall on fluid flow and thermal properties in a shallow lid-driven cavity and found that the highest local heat transfer rate occurred at the initial area of the lid

and decreased along the lid in the direction of the fluid flow. Zhang (2003) similarly examined the numerical simulation of a two-dimensional lid-driven square cavity and compared his own results with those of previous research.

Very little research has studied mixed convection with a lid-driven cavity. Tiwari and Das (2007) investigated numerically heat transfer enhancement in a lid-driven square cavity filled with a nanofluid. On the basis of the movement of the walls in different directions, they supposed three cases to study the effect of wall movements on the fluid flow and heat transfer in the cavity. The assisting and opposing mechanisms of mixed convection in a lid-driven cavity with moving vertical wall are being highlighted by Aydin (1999), who defined three flow regimes as (1) forced convection ($Ri < 0.1$), (2) mixed convection ($0.1 < Ri < 10$), and (3) natural convection ($Ri > 10$). Muthtamilselvan et al. (2009) also made a numerical investigation of the mixed convection in a lid-driven cavity and used copper–water nanofluid for different aspect ratios.

Moallemi and Jang (1992) investigated the impact of the Prandtl number (Pr) on the heat transfer improvement on a bottom-heated cavity and found that the impact of buoyancy was more significant for high values of Pr. They proposed a correlation for the average Nusselt number (Nu) with Pr, Re, and Ri numbers. Ji et al. (2007) carried out numerical and experimental studies on transient mixed convection and indicated that the temperature field showed a weak oscillatory trend at the initial, middle, and upper parts of the cavity. Prasad and Das (2007), in another work, examined different cases of moving walls maintained at different temperatures.

As can be seen in the preceding studies, often a cavity is studied in a horizontal position, whereas in practical industrial design applications, it is necessary to take into account the inclination of a cavity as the resulting lid-driven shear may assist or oppose buoyancy. Also, most existing studies where cavity inclination is considered have used base fluids and not nanofluids. Another point worthy of attention is that, in almost all studies presented so far on double lid-driven cavities, the movements of opposite walls are considered, while in engineering applications, movement of adjacent walls is also important. To meet some of these challenges, in this study, numerical analysis of mixed convective flow in a square double lid-driven cavity with moving adjacent walls is carried out, where the boundary conditions include a cooled right moving wall, with a heating fixed left wall, while the other walls are insulated. The results obtained are presented in streamline, temperature field format, obviously different from those of a horizontal cavity position. It must be noted that in continuance of the present study, the effect of a nanofluid with variable properties, the effect of an external magnetic and electric field, and unsteady phenomena will be considered and investigated.

2. MATHEMATICAL MODELING

A schematic of the double lid-driven cavity considered in the present study is shown in Fig. 1 with the boundary conditions and coordinates as indicated. The fluid in the

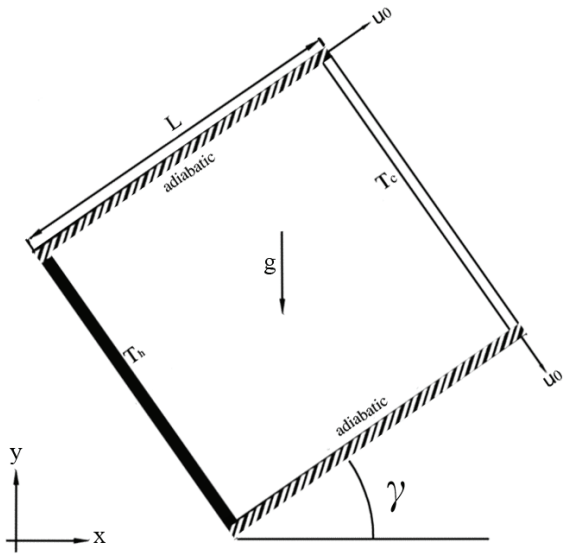

FIG. 1: Schematic of the double lid-driven cavity considered in the present study

cavity is water-based nanofluid containing copper nanoparticles that are assumed to be uniform in shape with equivalent diameter of 90 nm. As can be seen, the bottom and top walls are insulated, while the left and right walls are maintained at hot and cold temperatures, respectively. The top and left walls move with uniform velocity (u_0) and gravity acts vertically downward. Nanofluid is assumed Newtonian, with the flow being laminar and incompressible. Furthermore, base fluid and nanoparticles are assumed to be in thermal equilibrium with no slip between them. The thermophysical properties of the nanofluid are assumed constant, except for a variation of the density, which is approximated by the Boussinesq model, and those of Cu nanoparticles (90 nm) and water as base fluid are also presented in Table 1.

The governing equations for a steady, two-dimensional laminar and incompressible flow are expressed as follows:

$$\frac{\partial u}{\partial x} + \frac{\partial v}{\partial y} = 0 \ , \tag{1}$$

$$u\,\frac{\partial u}{\partial x} + v\,\frac{\partial u}{\partial y} = -\,\frac{1}{\rho_{nf}}\,\frac{\partial p}{\partial x} + \upsilon_{nf}\nabla^2 u \ , \tag{2}$$

$$u\,\frac{\partial v}{\partial x} + v\,\frac{\partial v}{\partial y} = -\,\frac{1}{\rho_{nf}}\,\frac{\partial p}{\partial y} + \upsilon_{nf}\nabla^2 v + \frac{(\rho\beta)_{nf}}{\rho_{nf}}\,g\Delta T \ , \tag{3}$$

TABLE 1: Thermophysical properties of water and copper

Property	Water	Copper
C_p	4179	383
ρ	997.1	8954
k	0.6	400
β	$2.1 \cdot 10^{-4}$	$1.67 \cdot 10^{-5}$
d_p (nm)	–	90

$$u\frac{\partial T}{\partial x} + v\frac{\partial T}{\partial y} = \alpha_{nf}\nabla^2 T \ . \tag{4}$$

The dimensionless parameters may be presented as follows:

$$\begin{gathered} X = \frac{x}{L}, \quad Y = \frac{y}{L}, \quad V = \frac{v}{u_0}, \quad U = \frac{u}{u_0} \\ \Delta T = T_h - T_c, \quad \theta = \frac{T - T_c}{\Delta T}, \quad P = \frac{p}{\rho_{nf} u_0^2} \end{gathered} \ . \tag{5}$$

Hence

$$\mathrm{Re} = \frac{\rho_f u_0 L}{\mu_f}, \quad Ri = \frac{Ra}{\mathrm{Pr} \cdot \mathrm{Re}^2}, \quad Ra = \frac{g\beta_f \Delta T L^3}{\upsilon_f \alpha_f}, \quad \mathrm{Pr} = \frac{\upsilon_f}{\alpha_f} \ . \tag{6}$$

The dimensionless forms of the preceding governing equations (1)–(4) become

$$\frac{\partial U}{\partial X} + \frac{\partial V}{\partial Y} = 0 \ , \tag{7}$$

$$U\frac{\partial U}{\partial X} + V\frac{\partial U}{\partial Y} = -\frac{\partial P}{\partial X} + \frac{\upsilon_{nf}}{\upsilon_f}\frac{1}{\mathrm{Re}} .\nabla^2 U \ , \tag{8}$$

$$U\frac{\partial V}{\partial X} + V\frac{\partial V}{\partial Y} = -\frac{\partial P}{\partial Y} + \frac{\upsilon_{nf}}{\upsilon_f}\frac{1}{\mathrm{Re}} .\nabla^2 V + \frac{Ri}{\mathrm{Pr}} . \frac{\beta_{nf}}{\beta_f}\Delta\theta \ , \tag{9}$$

$$U\frac{\partial \theta}{\partial X} + V\frac{\partial \theta}{\partial Y} = \frac{\alpha_{nf}}{\alpha_f}\nabla^2\theta \ . \tag{10}$$

Thermal diffusivity and effective density of the nanofluid are, respectively,

$$\alpha_{nf} = \frac{k_{nf}}{(\rho c_p)_{nf}} , \tag{11}$$

$$\rho_{nf} = \varphi\rho_s + (1 - \varphi)\rho_f . \tag{12}$$

Heat capacity and thermal expansion coefficient of the nanofluid are therefore, respectively,

$$(\rho c_p)_{nf} = \varphi(\rho c_p)_s + (1 - \varphi)(\rho c_p)_f , \tag{13}$$

$$(\rho\beta)_{nf} = \varphi(\rho\beta)_s + (1 - \varphi)(\rho\beta)_f . \tag{14}$$

The effective viscosity of nanofluid was proposed by Brinkman (1952) as follows:

$$\mu_{nf} = \frac{\mu_f}{(1 - \varphi)^{2.5}} . \tag{15}$$

The effective thermal conductivity of the nanofluid is calculated by the Maxwell model (Maxwell, 1904):

$$\frac{k_{nf}}{k_f} = \frac{k_s + 2k_f - 2\varphi(k_f - k_s)}{k_s + 2k_f + \varphi(k_f - k_s)} . \tag{16}$$

The Nusselt number can be calculated as follows:

$$Nu = \frac{hL}{k_f} , \tag{17}$$

where the heat transfer coefficient h is defined as

$$h = \frac{q_w}{T_h - T_c} \tag{18}$$

and the thermal conductivity may be expressed as

$$k_{nf} = \frac{-q_w}{\frac{\partial T}{\partial X}} . \tag{19}$$

By substituting Eqs. (18) and (19) into Eq. (17), the Nusselt number for the left hot wall can be written as

$$Nu = -\left(\frac{k_{nf}}{k_f}\right)\left(\frac{\partial\theta}{\partial x}\right) . \tag{20}$$

The average Nusselt number calculated over the hot surface by Eq. (18) becomes

$$Nu_m = \frac{1}{L}\int_0^L Nu dY \ . \tag{21}$$

The boundary conditions as set out earlier may be mathematically presented as

Left wall:

$$\begin{Bmatrix} U = V = 0 \\ \theta = 1 \end{Bmatrix} .$$

Right wall:

$$\begin{Bmatrix} U = 0,\ V = -1 \\ \theta = 0 \end{Bmatrix} .$$

Bottom wall:

$$\begin{Bmatrix} U = V = 0 \\ \dfrac{\partial \theta}{\partial Y} = 1 \end{Bmatrix} .$$

Top wall:

$$\begin{Bmatrix} U = 1,\ V = 0 \\ \dfrac{\partial \theta}{\partial Y} = 0 \end{Bmatrix} . \tag{22}$$

3. NUMERICAL METHOD

Governing equations for continuity, momentum, and energy equations associated with the boundary conditions in this study were calculated numerically based on the finite volume method and associated staggered grid system, using FORTRAN computer code. The SIMPLE algorithm is used to solve the coupled system of governing equations. The convection terms are approximated by a combination of the central difference scheme and the upwind scheme (hybrid scheme), which is conducive to a stable solution. Furthermore, a second-order central differencing scheme is utilized for the diffusion terms (Patankar, 1980). The algebraic system resulting from numerical discretization was calculated using the tridiagonal matrix algorithm applied in a line going through all volumes in the computational domain. The solution procedure is iterated until the following convergence criterion is satisfied:

$$error = \frac{\sum_{j=1}^{j=M}\sum_{i=1}^{i=N}\left|\lambda^{n+1} - \lambda^{n}\right|}{\sum_{j=1}^{j=M}\sum_{i=1}^{i=N}\left|\lambda^{n+1}\right|} < 10^{-7} \tag{23}$$

TABLE 2: Grid independence study for a nanofluid

Grid size	NU_{ave}
21 × 21	1.1838
31 × 31	1.3221
41 × 41	1.3736
51 × 51	1.4055
61 × 61	1.4273
71 × 71	1.4398
81 × 81	1.4452
91 × 91	1.4487
101 × 101	1.4504

Here M and N correspond to the number of grid points in the x and y directions, respectively, and λ denotes any scalar transport quantity. To verify grid independence, numerical procedure was carried out for nine different mesh sizes, namely, 21 × 21, 31 × 31, 41 × 41, 51 × 51, 61 × 61, 71 × 71, 81 × 81, 91 × 91, and 101 × 101. Average Nu of the bottom hot wall is obtained for each grid size, as shown in Table 2. As can be observed, an 81 × 81 uniform grid size yields the required accuracy and was hence applied for all simulation exercises in this work, as presented in the following section.

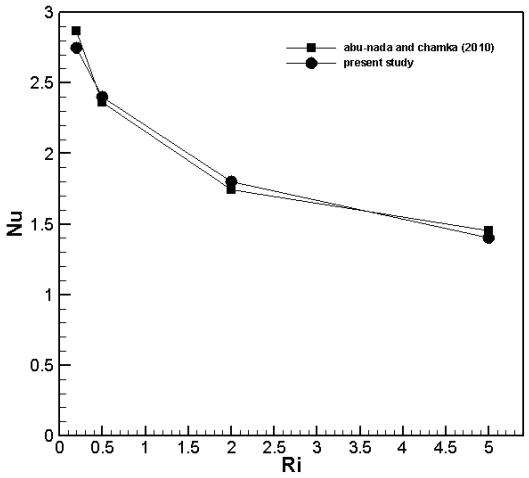

FIG. 2: Comparison of solutions for a cavity filled with nanofluid

TABLE 3: Comparison of solutions for natural convection in an enclosed cavity

	Present study	Mohammad and Viskanta (1992)	Ha and Jung (2000)	Abu-Nada and Chamkha (2010)
$Ra = 10^3$				
Nu	1.1366	1.0871	1.085	1.072
Nu_{max}	1.5738	1.508		
Nu_{min}	0.6468	0.6901		
$Ra = 10^4$				
Nu	2.3256	2.195	2.1	2.070
Nu_{max}	3.5456	3.5585		
Nu_{min}	0.7172	0.5809		
$Ra = 10^5$				
Nu	4.4928	4.450	4.361	4.464
Nu_{max}	7.3037	7.9371		
Nu_{min}	0.9906	0.7173		
$Ra = 10^6$				
Nu	8.6388	8.803		
Nu_{max}	14.2521	19.2675		
Nu_{min}	1.6247	0.9420		

The proposed numerical scheme was validated using the numerical results published by other researchers (Shahie et al., 2010; Fusegi et al., 1991; Ha and Jung, 2000) for a top heated moving lid and bottom cooled square cavity filled with air (Pr = 0.71). Applying the 81× 81 uniform mesh size, computations were carried out for 15 different Re and Gr combinations. Comparisons of average Nu at the hot lid are presented in Table 3, where an excellent agreement is confirmed, ensuring the validation. To ensure that the accuracy of the code is finalized, the results were compared with another study carried out by Abu-Nada and Chamkha (2010) in nanofluid, as shown in Fig. 2.

4. DISCUSSION

The Richardson number, $Ri = Gr/Re^2$, is the main parameter in mixed convection, providing a measure of importance for buoyancy-driven natural convection relative to the lid-driven forced convection. The effects of Ri, φ, and the enclosure inclina-

tion angle (γ) on the flow and temperature fields are investigated here. To obtain the required Ri, at fixed Gr = 10^4, Re is varied by changing the lid velocity u_0. Therefore, in this study, parameters studied include Ri ranging from 0.001 to 10, the velocity ratio ranging from 0.1 to 2.0, the cavity inclination angle γ ranging from 0º to 90º, and φ ranging from 0 to 0.1 at Gr = 10^4 and d_p= 90 nm.

Figures 3–6 present streamline and isotherm counters on the left and right columns, respectively, for various values of Ri and γ at φ = 0% (solid line) and φ = 8% (dashed line). As can be seen, as Ri increases, buoyancy-driven natural convection becomes more significant relative to the lid-driven forced convection. For lower Ri of about 0.001, in Figs. 3a, 4a, 5a, and 6a, the impact of the lid-driven flow dominates that of natural convection. In fact, streamline behaviors in the two-dimensional double lid-driven cavity discussed here could be characterized by a primary recirculating cell occupying most of the cavity generated by the moving lids and two secondary eddies near the left hot wall corners, with the one near the bottom corner being bigger and stronger than that in the top corner of the cavity. The isotherms are also clustered heavily near the left surface of the cavity, indicating steep temperature gradients in the horizontal direction in this region. In the remaining area of the cavity, the temperature gradients are weak, and this implies that the temperature differences are very small in the interior region of the cavity due to the vigorous effects of the mechanically driven circulations. It is interesting to note that, in this study, as the cavity inclination increases, little change occurs in the flow and isotherm patterns. Furthermore, various values of φ for the nanofluid do not seem to have a considerable effect on the flow patterns, perhaps because of the significance of the buoyancy effect. For instance, increasing φ from zero to 8% generates a negligible decrease in Ψ_{max} (i.e., from 0.1233 to 0.1134), which indicates that the presence of nanoparticles in such a range of φ causes the fluid to move slightly slower in the enclosure. However, changes in the temperature distribution as indicated in the isotherm contour plots are fairly significant compared to the case of pure water, indicating the significant improvement achieved in heat transfer (about 19.5% in the horizontal position) within the enclosure due to the presence of nanoparticles (φ = 8%) in the base fluid.

Figures 3b, 4b, 5b, and 6b present the streamlines and isotherms at Ri = 1 for φ = 0% and φ = 8% at inclination angle of 0º, 30º, 60º, and 90º, respectively. As expected at Ri = 1, these figures confirm that the buoyancy effect due to temperature gradient is comparable to shear effects due to a sliding lid. Increasing Ri from 0.001 to 1.0 has caused the disappearance of the two secondary eddies on the left corners of the cavity at all inclination angles, except γ = 90º, where one eddy reappears, be it weaker. At γ = 90º, the appearance of a secondary eddy at the bottom left corner could be contributed to opposing effects of buoyancy and shear forces, leading to reduced heat transfer within the cavity.

The streamlines flow primarily clockwise, circulating in a cell formed by the movement of the lid, which generally occupies the whole cavity space. The main

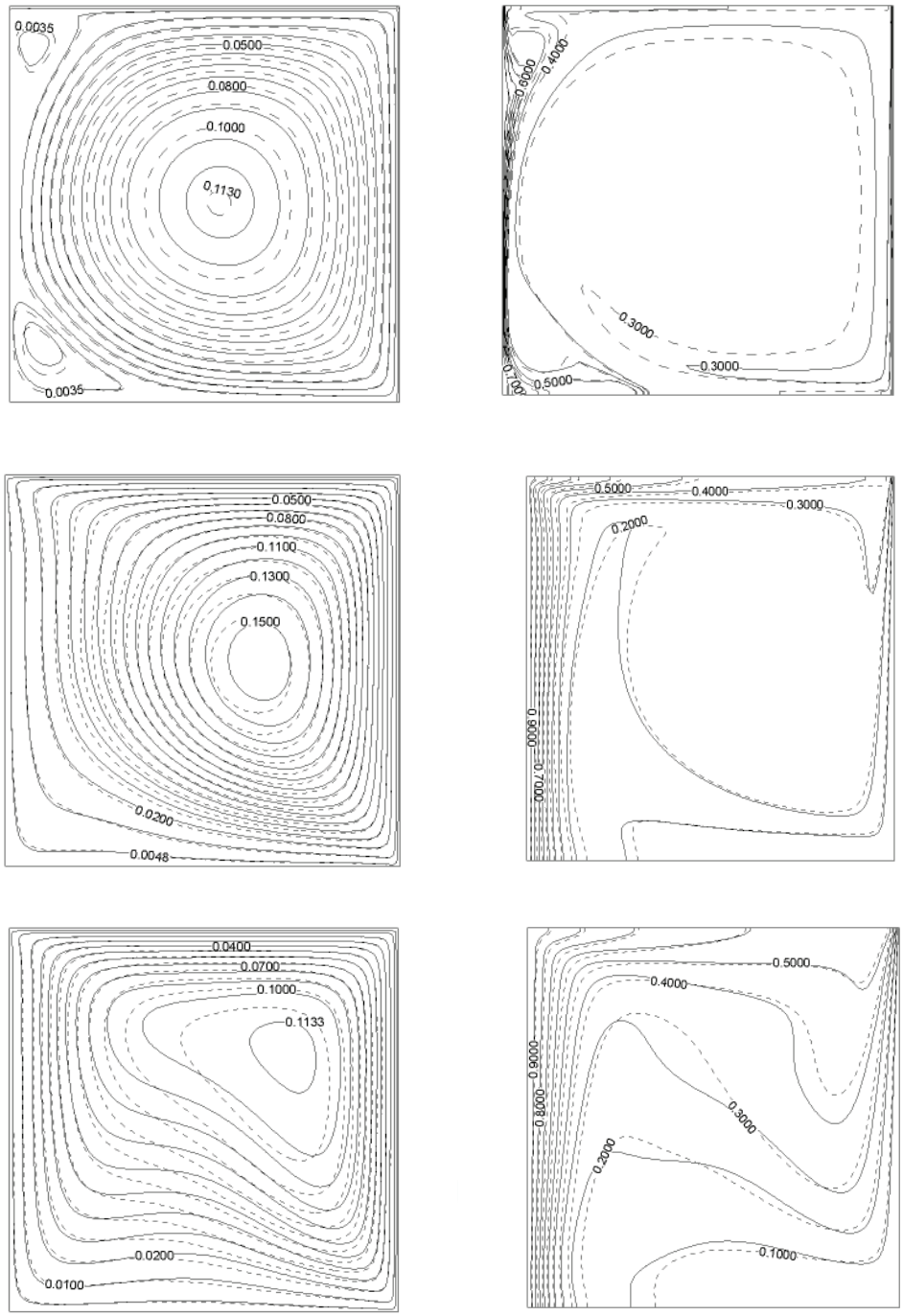

FIG. 3: Variation of streamlines (left) and isotherms (right) of the nanofluid (dashed lines) (solid lines) with Richardson number (a) Ri = 0.001, (b) Ri = 1, and (c) Ri = 10 and with $\gamma = 0$

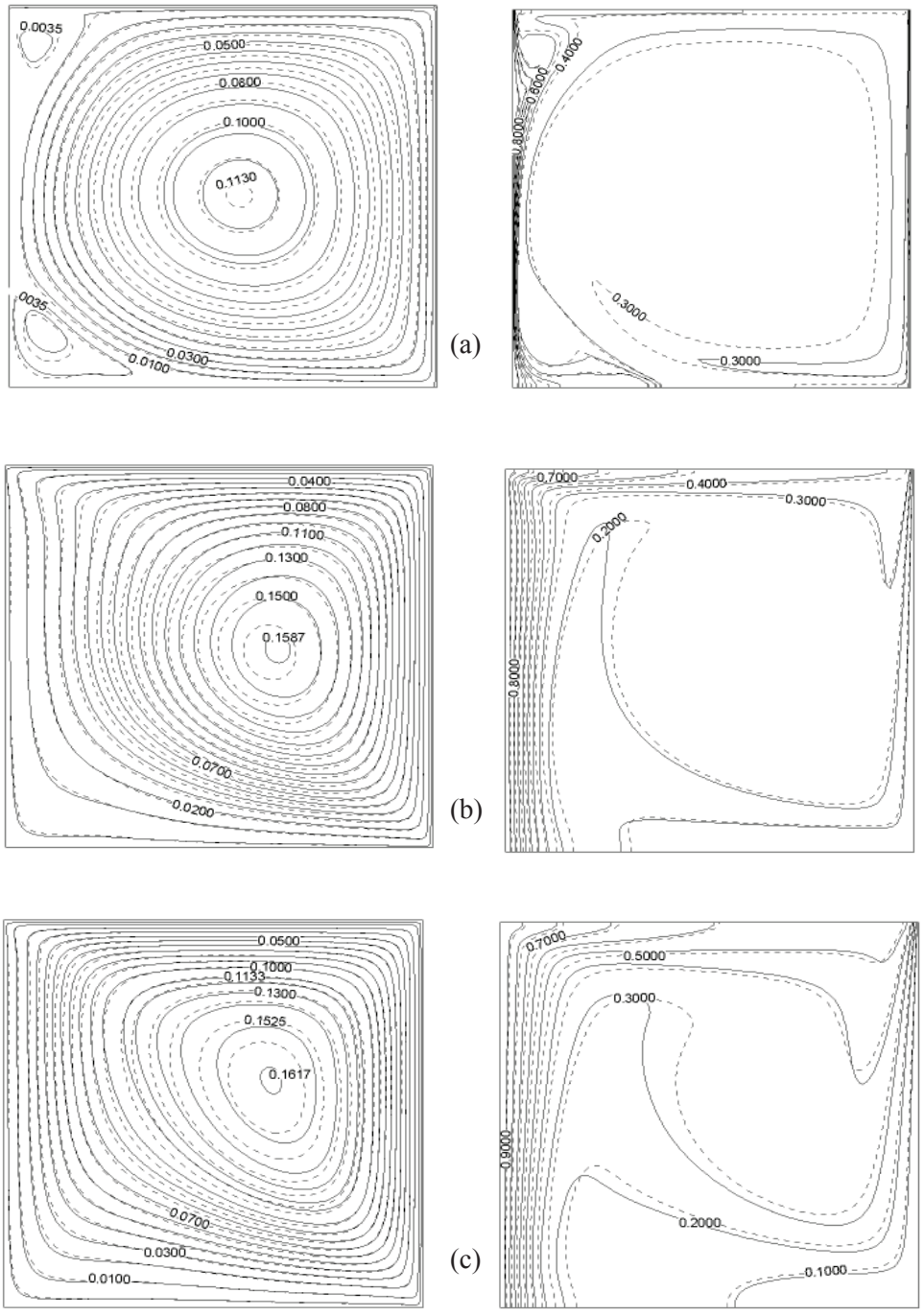

FIG. 4: Variation of streamlines (left) and isotherms (right) of the nanofluid (dashed lines) (solid lines) with Richardson number (a) Ri = 0.001, (b) Ri = 1, and (c) Ri = 10 and with $\gamma = 30$

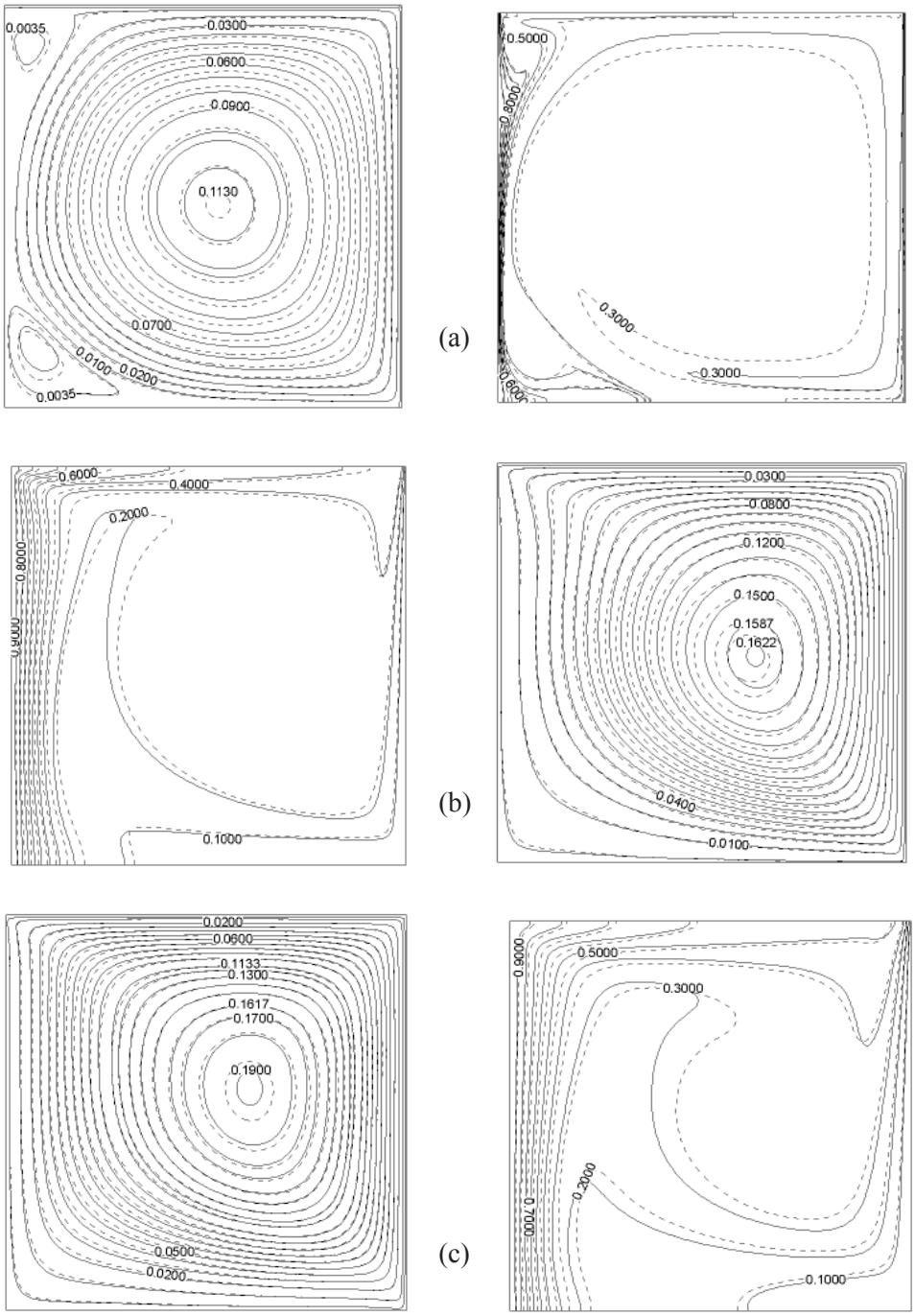

FIG. 5: Variation of streamlines (left) and isotherms (right) of the nanofluid (dashed lines) (solid lines) with Richardson number (a) Ri = 0.001, (b) Ri = 1, and (c) Ri = 10 and with $\gamma = 60$

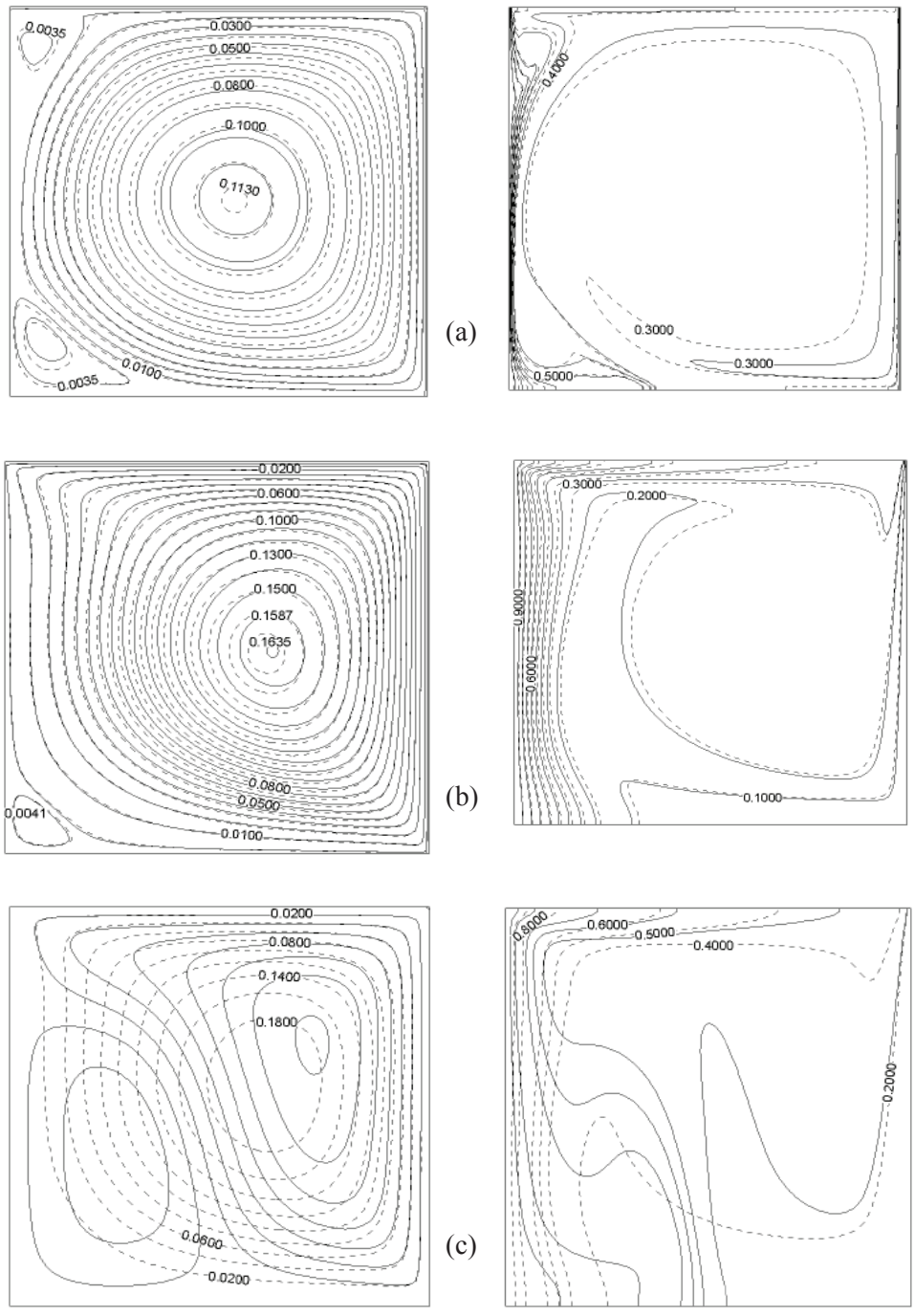

FIG. 6: Variation of streamlines (left) and isotherms (right) of the nanofluid (dashed lines) (solid lines) with Richardson number (a) Ri = 0.001, (b) Ri = 1, and (c) Ri = 10 and with $\gamma = 60$

cell core moves upward to the left top corner. The isotherms, however, spread out from the hot left wall, indicating moderate temperature gradients in the horizontal direction. Conversely, increasing γ to 90º causes Ψ_{max} to increase by about 8% without making any significant change in the patterns of the isotherm contours. Also, addition of nanoparticles (φ = 0.08) has produced small variations on the flow pattern, while it augments the flow intensity as Ψ_{max} increases from 0.1553 to 0.1585.

Increasing Ri to 10 indicates increased buoyancy force or natural convection within the cavity, as shown in Figs. 3c, 4c, 5c, and 6c for various values of γ, as indicated earlier. Streamlines do not seem to have altered due to the increase in Ri. However, for γ = 90º, drastic change takes place in streamlines for pure fluid, where another anticlockwise weaker cell is produced (see Fig. 6c) at the lower left corner.

It is interesting to note that for this inclination, the nanofluid flow pattern did not produce any secondary cell or any significant change with respect to other inclination angles. This vivid difference might be due to nanofluid helping in minimizing the natural convection effect. Compared to pure fluid, Ψ_{max} also shows an increase of 39% for nanofluid (from 0.1429 to 0.1987).

There is also a remarkable change in the isotherm pattern in the presence of nanoparticles (φ = 0.08) for γ = 90º compared to pure fluid. It is worth noting that, in this case, the presence of nanofluid improved heat transfer by about 36% compared to the base fluid, which is the highest improvement among all cases considered in this study.

In this case (Ri = 10), the isotherms spread further toward the right side, showing much more distortion than the isotherms corresponding to Ri = 1. Similar to the case of Ri = 1, except Fig. 6c, inclining the enclosure results in flow retardation and decreased temperature gradients along the left hot wall of the enclosure.

Variation of the local Nusselt number along the hot wall is plotted in Fig. 7 for all Richardson numbers. The effect of the presence of nanoparticles on the heat transfer process is clearly discernible in these plots. It is obvious that the Nusselt number at the hot lid starts with a small value at the bottom point and increases gradually to a high value toward the top point and then suddenly decreases.

In Fig. 7a, which is about variation of local Nusselt number at Ri = 0.001, it is observed that local Nusselt number increases from down to the top of the wall initially and then decreases severely. This decrease is because of the existence of two vortices in lower and upper corners of the hot wall. In Fig. 7b, Ri = 1, and Fig. 7c, the highest Richardson number considered, the local Nusselt number in the lower portion of the hot wall has a medium and a high value, respectively. As can be seen in Fig. 3 at Ri = 10, the buoyancy force is stronger than the shear force, and only a primary eddy is observed in the cavity. Therefore, by movement of the upward fluid along the hot wall and an increase in its temperature, the local Nusselt number increases.

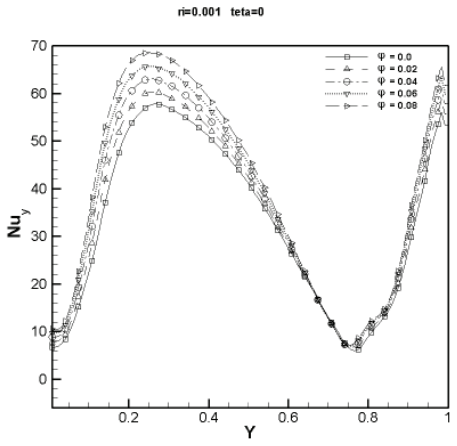

(a)

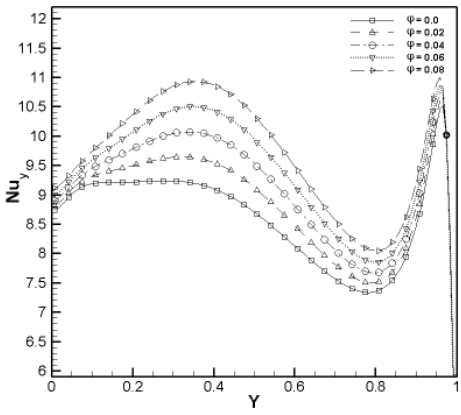

(b)

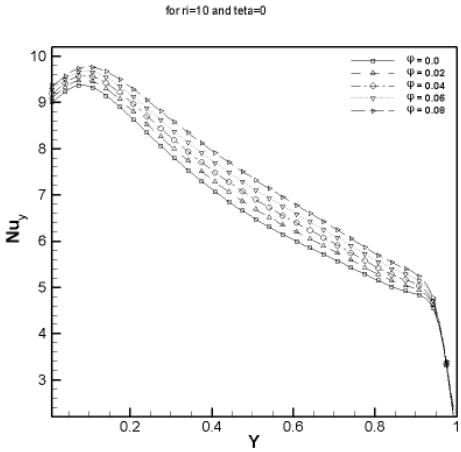

(c)

FIG. 7: Variation of local Nusselt number along the hot wall of the cavity with volume fraction of nanoparticles with (a) Ri = 0.01, (b) Ri = 1, and (c) Ri = 10 and with $\gamma = 0$

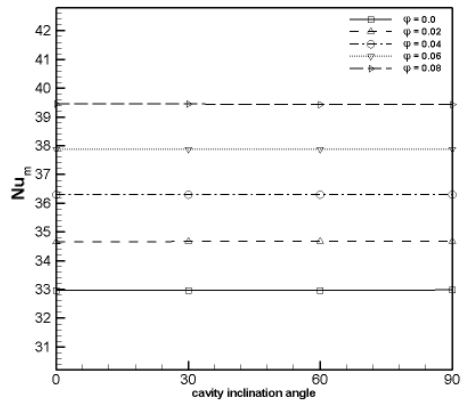

(a)

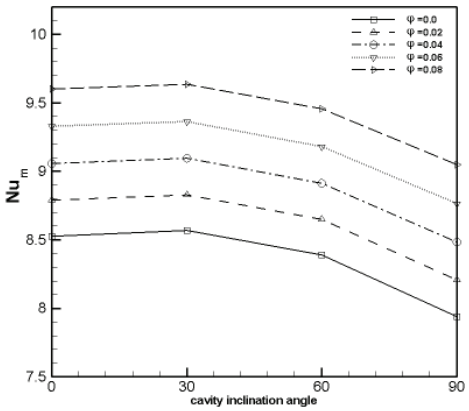

(b)

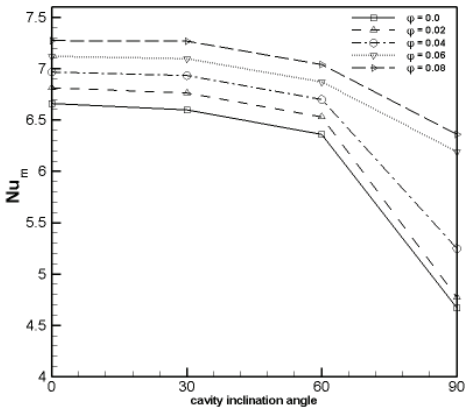

(c)

FIG. 8: Variation of the average Nusselt number of the hot wall with volume fraction of the nanoparticles and inclination angle of the cavity with (a) Ri = 0.001, (b) Ri = 1, and (c) Ri = 10

From the viewpoint of the use of the nanofluid, it can be seen from the figure that for all considered cases by an increase in the volume fraction of nanoparticles, the local Nusselt number increases significantly.

The effect of solid concentration on the variation of the average Nusselt number at the left hot wall is shown in Fig. 8. It is observed that for a given Richardson number, the average Nusselt number increases with an increase in solid concentration. This arises from the fact that physical properties of nanofluid change with volume fraction results in better heat transfer. It can be seen that the increase in solid concentration

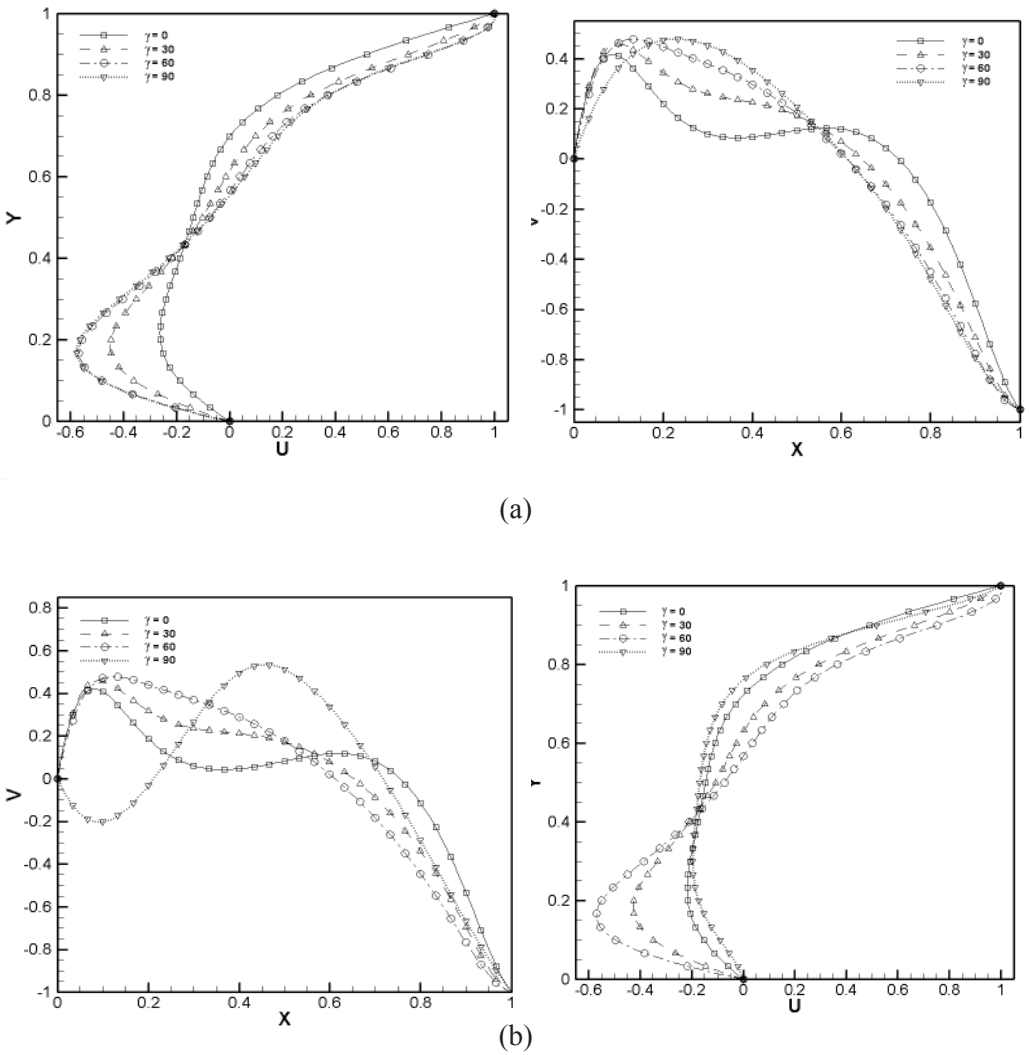

FIG. 9: Variation of horizontal (left) and vertical (right) components of velocity along centerlines of the cavity for different inclination angles at Ri = 10 for (a) pure fluid and (b) nanofluid with φ = 8%

has more effect on the average Nusselt number at higher Ri, so that by increasing solid concentration up to 8%, the average Nusselt number increases by about 19.7% for Ri = 0.001, about 12.6% for Ri = 10, and about 9.2% for Ri = 10 with a horizontal position of the cavity.

This is due to the fact that the conduction mode has more effect at lower Richardson number. So the increase in solid concentration, which enhances the effective thermal conductivity, plays a more effective role in lower Richardson number. It is obvious from these figures that an increase in cavity inclination angle causes a decrease in Nusselt number. Also, the increase in cavity inclination angles is more significant on the average Nusselt number at higher Ri, so that the decreases in Nu_m for 0.02 solid concentration are approximately 29.9% for Ri = 10 and 6.6% for Ri = 1, while for Ri = 0.001, it is less than 1%.

Figure 9 presents the typical x-component of velocity U at the vertical mid-plane of the enclosure, and the y-component of velocity V at the horizontal mid-plane of the enclosure for various values of the enclosure inclination angles for pure water ($\varphi = 0\%$) and nanofluid with $\varphi = 8\%$ at Ri = 10. It is observed from Fig. 9a that the x-component of velocity U decreases in the bottom part of the enclosure, whereas it increases in the upper part of the enclosure as the inclination angle increases. Conversely, as the inclination angle increases, the y-component of velocity V increases in the left part of the enclosure, whereas it decreases in the right part of the enclosure. In Fig. 9b (pure fluid), U and V behave exactly the same as in Fig. 8b, except for $\gamma = 90$.

5. CONCLUSIONS

In this investigation, results of numerical simulation of mixed convection heat transfer of the Cu–water nanofluid in double lid-driven inclined cavities are discussed. The finite volume method was employed for the solution of the present problem. Effect of parameters such as Ri number, solid concentration, and inclination angle of the cavity on the flow and temperature fields, as well as the heat transfer enhancement, are studied. Graphical and tabular results for various parametric conditions were presented and discussed. From this investigation, we can write the following conclusions:

1. This study was validated by a comparison with previously published work on special cases of the problem, and an excellent agreement was obtained.

2. The results demonstrated that for a particular Richardson number and Re, the increase in the solid volume fraction augments the heat transfer rate of the enclosure. The effect of solid volume fraction on heat transfer decreases by increasing the Richardson number.

3. Increase in solid concentration plays a more significant role in heat transfer with lower Richardson number.

4. For a given Ri, Re, and φ, increasing the cavity inclination angle leads to a decrease in heat transfer, mildly. Also, the increase in cavity inclination angle has a more effective role in heat transfer at higher Ri.

5. The temperature fields and total heat transfer are directly related to the presence of the vortices in the cavity.

6. Nanofluid helps in minimizing the natural convection effect. Also, nanoparticles are able to change the flow pattern of a fluid in natural convection dominant with respect to that of the pure fluid.

REFERENCES

Abu-Nada, E. and Chamkha, A. J., Mixed convection flow in a lid-driven inclined square enclosure filled with a nanofluid, *Eur. J. Mech. B Fluids*, vol. 29, pp. 472–482, 2010.

Aydin, O., Aiding and opposing mechanisms of mixed convection in a shear and buoyancy-driven cavity, *Int. Commun. Heat Mass Transfer*, vol. 26, pp. 1019–1028, 1999.

Basak, T., Roy, S., Sharma, P. K., and Pop, I., Analysis of mixed convection flows within a square cavity with uniform and non-uniform heating of bottom wall, *Int. J. Thermal Sci*., vol. 48, pp. 891–912, 2009.

Brinkman, H. C., The viscosity of concentrated suspensions and solutions, *J. Chem. Phys*., vol. 20, pp. 571–581, 1952.

Choi, S. U. S., Enhancing Thermal Conductivity of Fluids with Nanoparticles, *Proceedings of 1995 ASME Int. Mechanical Engineering*, *Congress and Exposition,* San Francisco, pp. 99–105, 1995.

Fusegi, T., Kuwahara, K., and Farouk, B., A numerical study of three-dimensional natural convection in a differentially heated cubic enclosure, *Int. J. Heat Mass Transfer*, vol. 34, no.6, pp. 1543–1557, 1991.

Guo, G. and Sharif, M. A. R., Mixed convection in rectangular cavities at various aspect ratios with moving isothermal sidewalls and constant flux heat source on the bottom wall, *Int. J. Thermal Sci.*, vol. 43, pp. 465–475, 2004.

Ha, M. Y. and Jung, M. J., A numerical study of three-dimensional conjugate heat transfer of natural convection and conduction in a differentially heated cubic enclosure with a heat-generating cubic conducting body, *Int. J. Heat Mass Transfer*, vol. 43, pp. 4229–4248, 2000.

Hwang, K.S., Lee, J. H., and Jang, S. P., Buoyancy-driven heat transfer of water-based Al_2O_3 nanofluids in a rectangular cavity, *Int. J. Heat Mass Transfer*, vol. 50, pp. 4003–4010, 2007.

Ji, T. H., Kim, S. Y., and Hyun, J. M., Transient mixed convection in an enclosure driven by a sliding lid, *Int. J. Heat Mass Transfer*, vol. 43, pp. 629–638, 2007.

Khanafer, K., Vafai, K., and Lightstone, M., Buoyancy-driven heat transfer enhancement in a two-dimensional enclosure utilizing nanofluids, *Int. J. Heat Mass Transfer*, vol. 46, pp. 3639–3653, 2003.

Lee, S., Choi, S. U. S., Li, S., and Eastman, J. A., Measuring thermal conductivity of fluids containing oxide nanoparticles, *J. Heat Mass Transfer*, vol. 121, pp. 280–289, 1999.

Masuda, H., Ebata, A., Teramae, K., and Hishinuma, N., Alteration of thermal conductivity and viscosity of liquid by dispersing ultra-fine particles (Dispersion of g-Al_2O_3, SiO2, and TiO_2 ultra-fine particles), *Netsu Bussei,* vol. 7, pp. 227–233, 1993.

Maxwell, J. C., *A Treatise on Electricity and Magnetism*, 2nd ed., Oxford: Oxford University Press, pp. 435–441, 1904.

Moallemi, M. K. and Jang, K. S., Prandtl number effects on laminar mixed convection heat transfer in a lid-driven cavity, *Int. J. Heat Mass Transfer*, vol. 35, pp. 1881–1892, 1992.

Mohammad, A. A. and Viskanta, R., Laminar flow and heat transfer in Rayleigh–Benard convection with shear, *Phys. Fluids A*, vol. 4, pp. 2131–2140, 1992.

Muthtamilselvan, M., Kandaswamy, P., and Lee, J., Heat transfer enhancement of copper–water nanofluids in a lid-driven enclosure, *Commun. Nonlinear Sci. Numer. Simul*., vol. 15, no. 6, pp. 1501–1510, 2009.

Ouertatani, N., Ben Cheikh, N., Ben Beyaa, B., Lilia, T., and Campo, A., Mixed convection in a double lid-driven cubic cavity, *Int. J. Thermal Sci.*, vol. 48, pp. 1265–1272, 2009.

Patankar, S. V., *Numerical Heat Transfer and Fluid Flow*, Washington, DC: Hemisphere, 1980.

Prasad, Y. S. and Das, M. K., Hopf bifurcation in mixed flow inside a rectangular cavity, *Int. J. Heat Mass Transfer*, vol. 50, pp. 3583–3598, 2007.

Shahie, M., Mahmoudi, A. H., and Talebi, F., Numerical study of mixed convective cooling in a square cavity ventilated and partially heated from the below utilizing nanofluid, *Int. J. Heat Mass Transfer*, vol. 37, pp. 201–213, 2010.

Tiwari, R.K. and Das, M.K., Heat transfer augmentation in a two-sided lid-driven differentially heated square cavity utilizing nanofluids, *Int. J. Heat Mass Transfer*, vol. 50, pp. 2002–2018, 2007.

Wen, D. and Ding, Y., Natural convective heat transfer of suspensions of titanium dioxide nanoparticles (nanofluids), *IEEE Transport Nanotechnol*., vol. 5, pp. 220–227, 2006.

Xuan, Y. and Li, Q., Heat transfer enhancement of nanofluids, *Int. J. Heat Fluid Flow*, vol. 21, pp. 58–64, 2000.

Zhang, J., Numerical simulation of 2D square driven cavity using fourth-order compact finite difference schemes, *Comput. Math. Appl*., vol. 45, pp. 43–52, 2003.